

INFLUENCE OF GRASSROOTS ON THE STABILITY OF SLOPES: EXPERIMENTAL MODELLING AND NUMERICAL ANALYSIS

*I Nengah Sinarta^{1,3}, Putu Aryastana¹, Kadek Windy Candrayana¹ and I Ketut Agung Sudewa²

¹Faculty of Engineering and Planning, Warmadewa University, Denpasar, Indonesia.

²Faculty of Agriculture, Warmadewa University, Denpasar, Indonesia.

³Master Program of Infrastructure and Environmental Engineering, Warmadewa University, Denpasar, Indonesia

*Corresponding Author, Received: 10 Oct. 2023, Revised: 15 Dec. 2023, Accepted: 16 Dec. 2023

ABSTRACT: Debris flow disasters were caused by surface erosion with high rainfall, especially in mountain villages on the island of Bali. This research aims to understand the stability behavior of volcanic soil due to physical and mechanical conditions based on numerical analysis with Plaxis 3D software. The experiment was used by planting in a test box in the form of a steel frame and equipped with a rainfall simulator to determine slope stability due to planting a combination of elephant grass and vetiver. Numerical results for volcanic soil conditions without vegetation show a soil tension of 0.6854 kN/m². Model results after four days, there was a decrease of 0.0001m, and after 33 days there was a decrease of 0.0000064 m for the slope 45°. The safety factor of slopes without vegetation is 0.8, so this condition has the threat of landslides and surface erosion. Experimental results show that adding elephant grass combined with vetiver grass can reduce erosion by 94.6% on slope 45° and 92.67% on slope 60°. The effectiveness of the resulting runoff reaches 55.48% on slope 45° and 53.89% on slope 60°. This increase in effectiveness was caused by the development of elephant grassroots, which spread horizontally, thereby increasing the bond with the top layer of soil.

Keywords: Bioengineering, Volcanic soil, Debris flow, Vetiver grass, Elephant grass

1. INTRODUCTION

Indonesia is a country that has a high potential for geological disasters due to tectonic conditions and tropical climate, and landslides and debris flows due to rainfall are a threat every year in mountainous and rural areas [1,2]. The area in Indonesia that frequently experiences landslides is the island of Bali. Heterogeneous morphological conditions consisting of hills and volcanoes cause high levels of landslides. Landslide disasters are ranked first compared to other disasters. Landslide disaster data states that in 2020, Bangli Regency experienced 27 landslides, or 16.26% of all landslides in Bali [3]. The debris flow that occurs is dominated by high rainfall, and in villages located on Mount Batur and Mount Abang, such as Trunyan Village, Abang Batudinding Village, and Buahon Village [4], debris flow triggers due to volcanic soil conditions with loose rocks, steep slopes, lack of vegetation, geological structure, high rainfall intensity, and long rain duration [5,6].

Erosion due to rain is a natural process that cannot be eliminated, so treating it by bioengineering concept was a sustainable practice [7,8]. Landslide and erosion mitigation using bioengineering concepts can be an option because it is cheap, environmentally friendly, and can be done independently [9]. The most widely used biotechnological treatment was planting grass because it can reduce soil surface erosion and is

more effective than trees [10–13] because bioengineering with trees will increase the load on the soil, which will have an impact on slope instability and can cause landslides [14,15]. The grass that was popularly used to overcome landslides was vetiver grass (*Vetiveria zizanioides*) because this plant was an annual plant that grows upright with a height of 1.5 – 2.5 m with a unique root system; its fibrous roots were able to penetrate very deep and reach a long distance, more than 3 meters and the record for the longest root was 5.2 meters, which was found in Doi Tung, Thailand [16]. Vetiver root penetration can increase the safety factor in terraced slopes [17]. Shear strength tests in the laboratory on soil samples with vetiver grass roots decreased with increasing water content—however, higher root length results in higher shear strength [18]. On sandy silt soils, vetiver grass reduces erosion by 94% - 97%, and soil erosion rates are reduced by up to 95%. Average surface runoff was also reduced by 21%, with root diameters from 1.6 to 2.5 mm, increasing soil erosion due to its negative impact on increasing additional cohesion [7].

Various previous studies depict Plaxis analysis as suitably used to determine debris flow involving large deformation. Utilizing the node-based smoothed point interpolation methods (NSPIMs) within the context of the particle finite element

method (PFEM), this research addresses substantial deformation challenges in geomechanics. This methodology facilitates the calculation of all variables at the nodes, thereby diminishing the necessity for frequent information transference, a common occurrence in PFEM, consequently augmenting efficiency. Despite encountering numerical instability challenges, the study proposes resolutions through two corrective techniques. The efficacy of this approach is corroborated through three numerical examples, demonstrating enhanced proficiency in the analysis of significant deformation problems [19]. The study concludes that the Material Point Method (MPM) is highly effective for modeling large deformation problems such as soil slope and earth dam failures under seismic loading. MPM overcomes the limitations of traditional mesh-based methods, particularly in capturing complex landslide processes and soil liquefaction. The method demonstrates significant potential in earthquake engineering, especially in understanding seismic slope failures and soil liquefaction mechanisms [20]. The enhanced version of NSPIMs, termed I-NSPIMs, has been effectively implemented for hydro-mechanical problems in geomechanics. Key modifications include the adoption of linear strain and simplified nodal smoothing domains. Evaluations through various case studies indicate that I-NSPIMs significantly improve accuracy and reduce numerical solution oscillations compared to the original NSPIMs, particularly in flow and flow-deformation problems. In conclusion, I-NSPIMs offer substantial improvements in performance and accuracy for coupled problems in geomechanics [21].

The current study aims to combine vetiver grass and elephant grass to increase soil strength against landslides. The idea of adding elephant grass is

aimed at reducing soil erosion. It is also hoped that the addition of elephant grass can be used as animal feed by residents around the planting location.

2. RESEARCH SIGNIFICANCE

The utilization of vetiver grass for water conservation and slope stability has been implemented in landslide-prone areas in East Bali, specifically in Ban Village [22]. However, it could not withstand surface runoff erosion due to its roots continuing underground. The current research aims to combine vetiver grass with elephant grass (*Pennisetum purpureum*), which has agar fibers on the surface to increase the ability of volcanic soil to resist erosion or debris flows, as well as animal feed. Volcanic soil originating from rock weathering needs to be analyzed based on physical and mechanical properties to determine the reliability behavior, so it is necessary to carry out numerical analysis with Plaxis 3D software to determine the stress, displacement, and safety factor of the soil at the age of 4 days and 33 days. At 4 days, the focus is on the initial root development, which is key for early soil stabilization. By 33 days, the grass typically reaches a mature phase with a developed root system and sufficient biomass, making it suitable for erosion control and potential use as livestock feed.

3. MATERIAL AND MODELING

The research used soil samples from Abang Batudinding Village (Fig. 1a), which is located on the slopes of Mount Abang, as shown in Fig. 1b. This location was chosen based on the tendency for landslides and high rainfall, and in 2020, this location experienced a landslide which caused two fatalities [23].

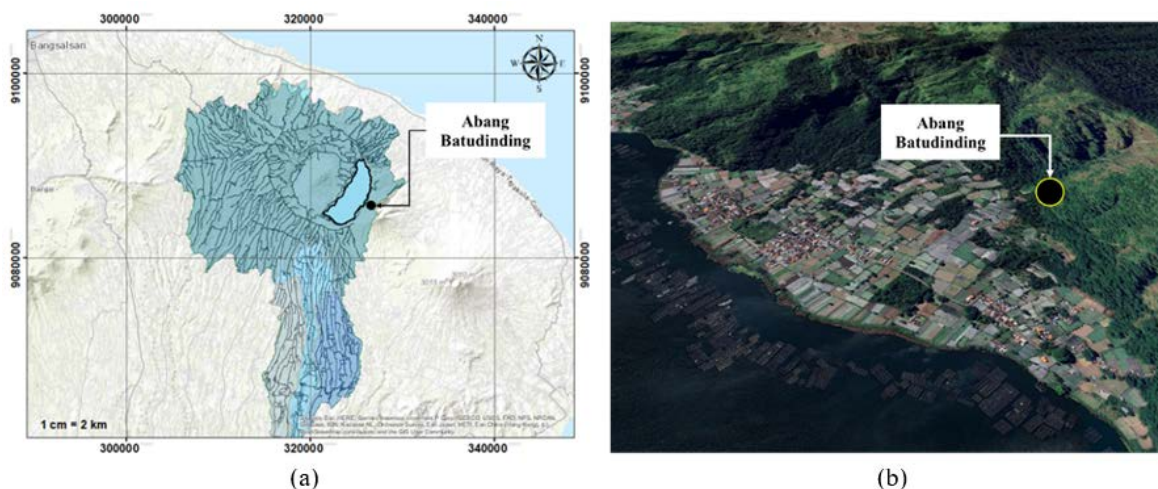


Fig. 1 (a) Location of Batudinding village, (b) Soil sampling location area

3.1 Soil Analysis

Soil property data was obtained by laboratory and field testing. Field testing was carried out using Boring and SPT (Standard Penetration Test), and laboratory testing. Test methods follow the American Society for Testing and Materials (ASTM) such as physical properties carried out on soil samples in the study area consisting of natural water content test (ASTM D-2216), density test (ASTM D-2937), specific test gravity (ASTM D-854), sieve analysis (ASTM D-136), to obtain values such as: degree of saturation (S_r), porosity (n), pore number (e), field density (γ_s), specific gravity (G_s) and dry density (γ_d). The mechanical properties of soil (soil shear strength) are directly shear and triaxial tests. The results of soil investigations show that the top soil layer was dominated by silty sand, and the layer below was silty sand with breccia fragments [14,11,16].

3.2 Rainfall Analysis

Analysis of rainfall forecasts in the research used rainfall data taken from the rainfall measuring post closest to the research location, namely Kintamani Post at coordinates 08°14'24 "LS - 155° 19'49" E. The rainfall data used was rainfall data for the last ten years from 2012 to 2021. The design rainfall used a return period of 25 years with rainfall of 69.76 mm as a result of the Pearson Log (Table 1). This rainfall was chosen because it is close to the

rainfall value at the time of the landslide in 2020 is 65.3 mm.

Table 1 Design Rainfall

Period	Log Pearson III Design Rainfall (mm)
1.01	16.59
2	44.63
5	56.92
10	63.27
25	69.76
50	73.73

3.3 Laboratory Model

The experiment model was made with a steel box with glass walls to see rooting and was able to form a slope of 45° and 60°, the slope variations adopted the average slope at the research location. The depth of the model is 3m, which aims to model layers from field test results. The soil layer in the model at a depth of 1m was filled with silty sand, and at further depths up to 3m, breccia fragments were added. Sand is added to the base layer of soil to encourage infiltration and can be measured in trays, as shown in Fig. 2a and Fig. 2b. The sides and front of the model use glass to observe root growth and see erosion and deformation of the slope surface.

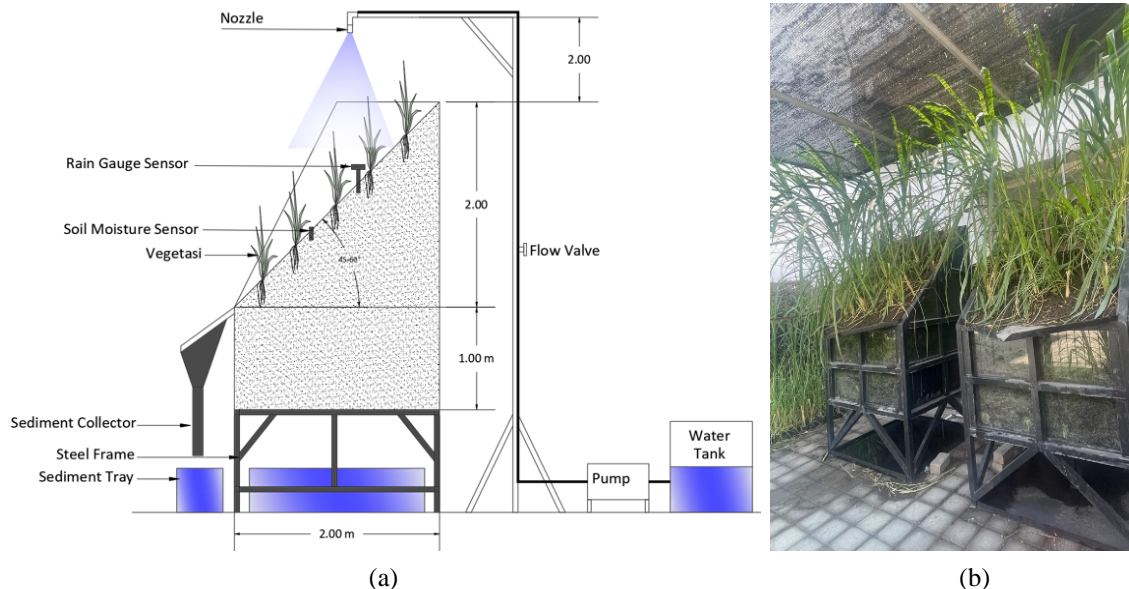


Fig. 2 (a) Section of box model, (b) Experiment box

The planting pattern in the experiment box was based on literature studies and observational purposes, initially testing only vetiver grass, as shown in Fig. 3a, and then modified by adding elephant grass as shown in Fig. 3b. The purpose of

adding elephant grass was to reduce surface erosion, where from observations of root development it was known that the distribution of elephant grass roots was able to bind the structure of the topsoil (topsoil) [24]. Table 2 shows the model scenario settings

consisting of 6 scenarios, where slope conditions are modeled without vegetation or bare soil, with vetiver vegetation, and a combination of vetiver and elephant grass.

Table 2 Model configuration

No	Model Code	Vegetation	Spacing (cm)	Slope (°)
1	BS1	None	0	45
2	BS2	None	0	60
3	V1	Vetiver	20	45
4	V2	Vetiver	20	60
5	VG1	Vetiver+ Elephant Gr	20	45
6	VG2	Vetiver+ Elephant Gr	20	60

The characteristics of the island of Bali in the form of mountains and coasts cause variations in rainfall [25]. Heavy rainfall with a duration of 4-6 hours is a common characteristic in Bali [26].

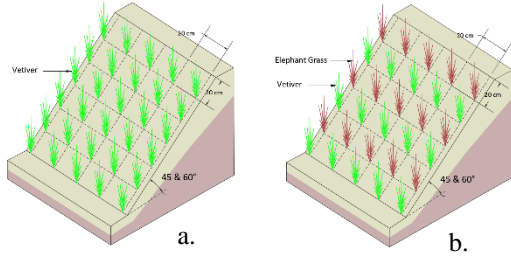


Fig. 3 Planting configuration

The rainfall model in the experiment uses a single spray nozzle installed in the center of the test box, the nozzle uses a stainless steel nozzle with a spray angle of 45°, and a hole diameter of 1.6 mm to achieve rainfall of 65-70 mm/hour [27]. These considering, it hoped that the pressure and water flow rate applied to the nozzle are suitable to produce droplets and achieve the desired rainfall intensity, control valves and pressure gauges were installed to achieve the design rainfall. Rainfall measurements using the Misol Weather Station, and calibrating rain readings using a manual ombrometer.

3.4 Numerical Modelling

The Prefabricated Vertical Drain (PVD) theory was an approach to analyzing settlement at the loading stage due to primary or initial soil consolidation. Consolidation theory is based on Terzaghi's one-dimensional consolidation theory, which can be formulated as:

$$\frac{\partial u}{\partial t} = c_v \frac{\partial^2 u}{\partial z^2}; c_v = \frac{kv}{m_v \gamma_w} \quad (1)$$

where C_v is the vertical consolidation coefficient, u is the excess pore pressure, t is the real time, z is the

position of the soil deposit, kv is the permeability coefficient in the vertical direction, m_v = vertical compression coefficient, and w is the unit weight of water. The equation is derived with the assumption that water dissipation only occurs in the vertical direction.

Water flows mainly in a horizontal direction because the distance between PVDs is shorter than the vertical direction of flow into the porous soil layer. The following theory of radial (horizontal) consolidation was proposed by Barron (1948):

$$\frac{\partial u}{\partial t} = c_h \left(\frac{\partial^2 u}{\partial r^2} + \frac{1}{r} \frac{\partial u}{\partial r} \right); c_h = \frac{kh}{m_v \gamma_w} \quad (2)$$

where Ch is the horizontal consolidation coefficient (m^2/s); kh = horizontal permeability coefficient. The combination of vertical and horizontal flow consolidation is derived from the proposed equation [28].

$$\frac{\partial u}{\partial t} = c_v \frac{\partial^2 u}{\partial z^2} + c_h \left(\frac{\partial^2 u}{\partial r^2} + \frac{1}{r} \frac{\partial u}{\partial r} \right) \quad (3)$$

The development of consolidation has been estimated by the average consolidation degree U . Initial pore pressure distribution and time factor data are used to calculate the degree of consolidation in the vertical direction. Meanwhile, the degree of radial consolidation was developed by Baron in 1948 as the following equation:

$$U_h = 1 - \exp \left[\frac{-8Th}{F_n} \right]; T_h = \frac{c_h t}{D^2} \quad (4)$$

where: t is the consolidation time; D is the unit diameter of the PVD influence area (m); F_n is the channel distance factor is $\ln(D/dw) - 3/4$; dw is the PVD equivalent diameter.

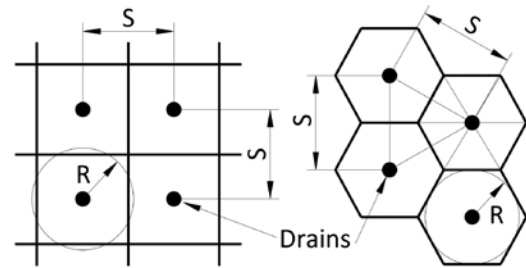


Fig. 4 PVD pattern (left: square pattern; right: triangle pattern) [21]

Generally, PVD was installed in a square or triangular pattern. With the area of influence, the rectangular equivalent diameter D is equal to $1.13 S$, and D is equal to $1.05 S$ for the triangular pattern, where S is the distance between the PVDs. The theory of consolidation with radial drainage assumes that water in the soil flows horizontally in a circular section towards the PVD. The radial consolidation equation considers the vertical drainage diameter (dw). This dw value is the diameter of the drainage column cylinder if the vertical drainage is made from a sand column. PVD tape is usually 100–120 mm wide and 3–6 mm thick.

The cross-section was not circular. Therefore, the equivalent area in a circle must be expressed in terms of the equivalent diameter, notation d_w . The equivalent diameter of the PVD is defined as the diameter of the drainage circle that has the same drainage capacity as the PVD in Fig. 4.

In many conditions, the equivalent diameter (d_w) can be considered independent of the condition of the subsoil, soil properties, and the influence of the PVD installation, but only depends on the drainage geometry and configuration. Fig.5 shows the mandrel used to install PVD in soft soil layers. It must be strong enough to prevent bending or buckling and soft soil will be analyzed in the smear zone as the zone is disturbed.

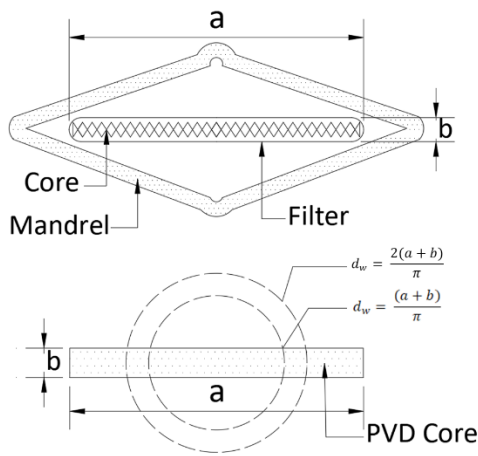


Fig. 5 (a) Cross section of PVD and mandrel, (b) PVD Equivalent Diameter [22]

In design, the equivalent diameter was determined by the surface area of the vertical channel in a circle that is the same or equivalent to the surface area of the vertical channel as estimated $\pi d_w = 2(a+b)$. So, the equivalent diameter is:

$$d_w = \frac{2(a+b)}{\pi} \quad (5)$$

where a is the typical width, b is the PVD thickness. Other researchers proposed d_w in Table 3 based on different considerations. The equation is considered as a throttle to control the drain [29]. The equation was created by considering the cross-sectional area of the PVD. The development of d_w was based on a similar discharge in an equivalent circular when subjected to pressure-controlled pumping conditions [30]. However, definitive recommendations were available regarding the validity of this equation.

Table 3. PVD equivalent diameter formula

Reference	Equivalent Equation
Hansbo	$d_w = \frac{2(b+\delta)}{\pi}$

Atkinson & Eldred

$$d_w = \frac{(b+\delta)}{\pi}$$

Fellenius & Castonguay

$$d_w = \sqrt{\frac{4b\delta}{\pi}}$$

Long & Covo

$$d_w = 0.5b = 0.7b$$

Abuel-Naga & Bouazza

$$d_w = 0.45b$$

4. RESULTS AND DISCUSSION

The results of soil testing and in the laboratory obtained data in the form of sandy silt soil with a small clay fraction, where this soil is the result of weathering of volcanic rocks. This sandy silt soil has non-plastic properties and high permeability values. Based on the table, it shows that volcanic soil tends to be sandy silt if it contains water has a soft consistency, and is very easily eroded.

Plaxis 3D software numerical analysis. in this study, a homogeneous slope with a height of 4 meters, a width of 4 meters, and a length of 4 meters is considered. Table 4 shows the parameters used in the slope analysis.

Table 4. Laboratory Results

	Description	Unit	Value
	Unit Weight (γ)	kN/m ³	16
	Modulus of Elasticity (E)	kPa	7500
Soil	Effective Poisson's ratio (ν)	-	0.35
(Mohr Coulomb model)	Effective Cohesion (c)	kPa	5
	Effective friction angle (ϕ)	(°)	30
	Incremental Cohesion (c')	kPa	15

Fig. 6 shows the slip plane stress based on slip plane patterns and surface erosion on volcanic soil slopes. The results show that in the model without vegetation the slip plane strain reaches 0.6854 kN/m². The results of the analysis of land movement or settlement due to erosion decrease over time because the soil creates new stability. Analysis of the formation of a new stability in 4 days where the maximum decrease was 0.0001 m and the decrease in 33 days with a maximum decrease of 0.0000064 m, this form proves that the results are correct behavior according to experimental testing if scaled in the model experimental = 0.01mm and 0.0064 mm, which

cannot be seen visually.

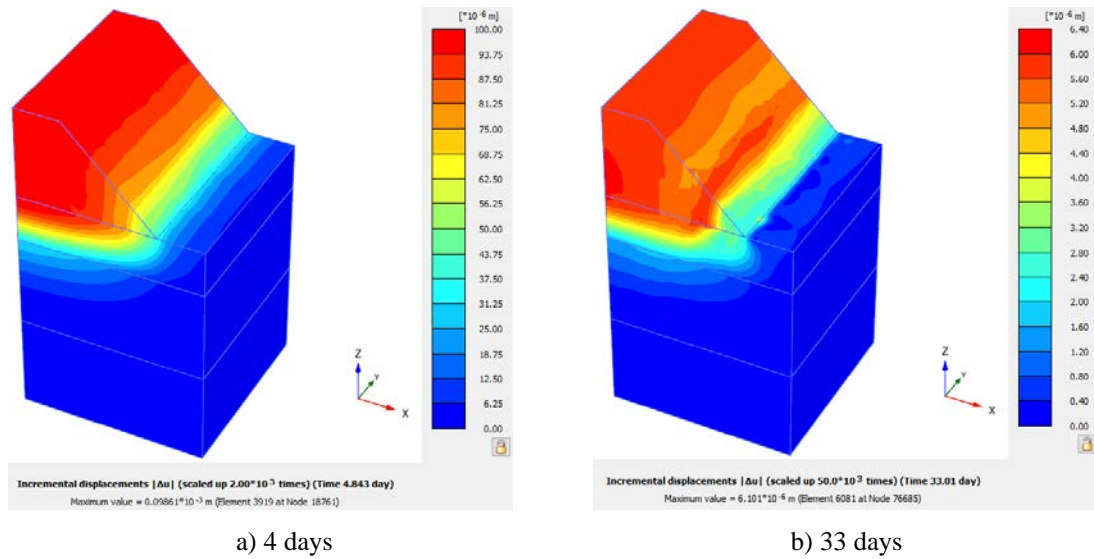


Fig. 6 Visual 3D Derivation

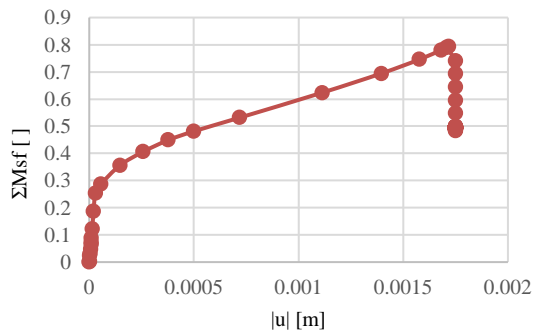


Fig. 7 Msf graph with decrease

Fig.7 shows a graph between total displacement and Incremental multipliers (Msf). The graph shows that the slope safety factor due to erosion was 0.80 without vegetation, so in this case, land without vegetation has the threat of landslides and eroding, even without the influence of rain.

4.1 Soil Erosion

Raindrops on to the soil surface cause erosion, and high-intensity rain produces higher kinetic energy, resulting in maximum erosion. Soil erosion was analyzed by weighing the sediment carried by rainwater. The test results showed that the effectiveness of adding vetiver grass vegetation (V1) was able to reduce soil erosion by up to 91.8% on a slope of 45°. The addition of elephant grass configurations can increase soil erosion reduction by up to 94.6%. However, on straighter slope conditions, namely 60°, the reduction rate decreases. The vetiver grass configuration (V2) decreased reduction ability to 90.6%, and the

addition of elephant grass was able to reduce erosion by 92.7% (Table 5).

Table 5 The effect of vegetation on erosion

No	Model Code	Slope (°)	Erosion (kg)	Reduction (kg)	Percentage of Reduction
1	BS1	45	10.78	0.000	0.0%
2	V1	45	0.880	9.900	91.8%
3	VG1	45	0.580	10.200	94.6%
4	BS2	60	11.89	0.000	0.0%
5	V2	60	1.120	10.770	90.6%
6	VG2	60	0.870	11.020	92.7%

4.2 Surface Runoff

This test was carried out after the roots of vetiver grass and elephant grass were 1 month (33 days) old. This aims to provide time for vegetation to bind to the topsoil and for maximum root development. Water runoff from the rainfall simulator is collected every 5-minute interval. A fiberglass container was installed at the end of the sediment collector. Runoff water consists of soil particles and is filtered through a filter with a paper surface. The test results show that vegetation was able to cut off rain so that less rain reaches the ground surface. The presence of vegetation reduces the speed of runoff, so soil erosion is reduced. There was an increase in the effectiveness of reducing runoff with the addition of elephant grass because the coverage of elephant grass was wider than vetiver grass. The addition of elephant grass on a 45° slope can reduce runoff by 55.48%. In the VG2 scenario on a slope of 60°, the ability to reduce runoff decreases to 53.89%. This

condition is caused by an increase in surface flow velocity due to increasingly steep slopes (Table 6).

Table 6 The effect of vegetation on surface runoff

No	Model Code	Slope (°)	Total Runoff (m) ³	Reduction (m) ³	Percentage of Reduction
1	BS1	45	0.099	0.000	0.00%
2	V1	45	0.058	0.041	41.41%
3	VG1	45	0.044	0.055	55.48%
4	BS2	60	0.105	0.000	0.00%
5	V2	60	0.064	0.040	38.53%
6	VG2	60	0.048	0.056	53.89%

The development of elephant grass, whose dominant roots grow horizontally, causes wider land cover. The runoff rate increases due to increasing rain duration, on slope 45°, planting vetiver grass (V1) was able to reduce runoff by 0.041 m³ or 41.41% according to the combination of elephant grass, there was an increase in runoff reduction of up to 0.055 m³ or 55.48%. The graph of the influence of elephant grass vegetation on surface runoff is as shown in Fig.8.

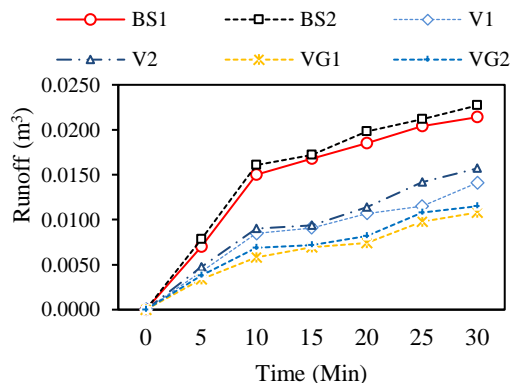


Fig. 8 The effect of vetiver grass and elephant grass on surface runoff

An analysis is crucial for providing a thorough evaluation of the effectiveness and sustainability of the proposed solution. This discourse should encompass the enduring impact of grassroots on soil cohesion and structure, the potential for sustained erosion control over prolonged periods, and the ongoing maintenance requirements of the grass. Furthermore, considering the ecological ramifications and the adaptability of the grass to fluctuating environmental conditions would significantly enrich the analysis. By addressing these elements, the study will furnish a more comprehensive understanding of the long-term advantages and challenges associated with grass planting as a method for soil stabilization, such as:

- (1) Implementation of natural mitigation using

- elephant grass for technical aspects in environmental engineering to prevent landslides.
- (2) Further development and refinement of similar methods in environmental engineering.
- (3) More in-depth research, including the exploration of plant species diversity.
- (4) Potential implications for research in areas with varied soil conditions.

5. CONCLUSION

This research begins with a numerical analysis using a volcanic soil model which shows the results of soil strain with slip patterns and surface erosion without vegetation of 0.6854 kN/m², and analysis of the formation of new stability within 4 days, a maximum decrease of 0.0001 m and a decrease of 0.0001 m. at 33 days it was 0.0000064 m, as well as displacement and Incremental multipliers (Msf), showing a slope safety factor due to erosion of 0.80 without vegetation. So, in this case, land without vegetation has the threat of landslides and erosion.

An experimental model of vetiver and elephant grass planting patterns as sustainable biotechnology to overcome landslides and vegetation debris flows on volcanic soil with vetiver grass and elephant grass can reduce the level of erosion due to surface runoff. The erosion rate with the vetiver grass configuration on slope 45° with a planting distance of 20 cm was 91.8%, and on slope 60° was 90.6%. The configuration of modifying vegetation by adding elephant grass can increase the soil's ability to resist soil loss due to surface runoff erosion by 94.6% on slope 45° and 92.67% on slope 60°. The effectiveness of adding vetiver grass and elephant grass in reducing surface runoff was 55.48% on slope 45° and 53.89% on slope 60°.

6. ACKNOWLEDGMENTS

We want to thank The Ministry of Education, Culture, Research and Technology of The Republic of Indonesia for financial support in the form of a 2023 fundamental research grant. Soil Mechanics Laboratory, Civil Engineering Department, Faculty of Engineering and Planning, Warmadewa University for granting permission to use this equipment. Our gratitude also goes to the Disaster Management Agency (BPBD) of the Bangli district, which provided access to research in the region.

7. REFERENCES

- [1] Sinarta I. N., Rifa'i A., Fathani T. F., and Wilopo W., Geotechnical properties and geological age on characteristics of landslides hazards of volcanic soils in Bali, Indonesia. International Journal of GEOMATE, Vol. 11, No. 26, 2016, pp. 2595–2599, doi: 10.21660/2016.26.67987.
- [2] Sinarta I. N., and Wahyuni P. I., Analisis potensi

- longsor rombakan (debris flow) dengan pemodelan aliran di lereng gunung Abang , Kintamani,Bali. Media Komunikasi Teknik Sipil, Vol. 28, No. 2, 2022, pp. 161–168.
- [3] Sinarta I. N., Rifa'i A., Fathani T. F., and Wilopo W., Spatial analysis of safety factors due to rain infiltration in the Buyan-Beratan ancient mountains. *International Review of Civil Engineering*, Vol. 11, No. 2, Mar. 2020, pp. 90–97, doi: 10.15866/IRECE.V11I2.17668.
- [4] Sinarta I. N., Rifa'i A., Fathani T. F., and Wilopo W., Slope stability assessment using trigger parameters and sinmap methods on Tamblingan-Buyan ancient mountain area in Buleleng regency,Bali. *Geosciences (Switzerland)*, Vol. 7, No. 4, 2017, doi: 10.3390/geosciences7040110.
- [5] Sinarta I. N., and Ariyana Basoka I. W., Safety factor analysis of landslides hazard as a result of rain condition infiltration on Buyan-Beratan ancient mountain safety factor analysis of landslides hazard as a result of rain condition infiltration on Buyan-Beratan ancient mountain. *Journal of Physics: Conference Series*, Vol. 1402, No. 2, 2019, doi: 10.1088/1742-6596/1402/2/022002.
- [6] Sinarta I. N., Wahyuni P. I., and Aryastana P., Analysis of debris flow hazard in volcanic soil by the flood flows modelling (dflowz) and nakayasu synthetic unit hydrograph. *International Review of Civil Engineering*, Vol. 14, No. 2, 2023, pp. 112–118, doi: 10.15866/irece.v14i2.20470.
- [7] Aziz S., and Islam M. S., Erosion and runoff reduction potential of vetiver grass for hill slopes: a physical model study. *International Journal of Sediment Research*, Vol. 38, No. 1, 2023, pp. 49–65, doi: 10.1016/j.ijsrc.2022.08.005.
- [8] Sinarta I. N., Penggunaan dan perkembangan konstruksi hijau untuk melindungi lereng. in *Seminar Nasional Refleksi 30 Tahun Fakultas Teknik*, Denpasar: Warmadewa University Press, 2014, pp. 248–254.
- [9] Islam M. S., Nasrin S., Islam M. S., and Moury F. R., Use of vegetation and geo-jute in erosion control of slopes in a sub-tropical climate. *International Journal of Civil, Environmental, Structural, Construction and Architectural Engineering*, Vol. 7, No. 1, 2013, pp. 31–39.
- [10] da Silva R. M., Santos C. A. ., and dos Santos J. Y. ., Evaluation and modeling of runoff and sediment yield for different land covers under simulated rain in a semiarid region of Brazil. *International Journal of Sediment Research*, Vol. 33, No. 2, 2018, pp. 117–125.
- [11] Ridzuan M. J. M., Abdul Majid M. S., Afendi M., Azduwin K., Amin N. A. M., Zahri J. M., and Gibson A. G., Moisture absorption and mechanical degradation of hybrid pennisetum purpureum/glass–epoxy composites. *Composite Structures*, Vol. 141, May 2016, pp. 110–116, doi: 10.1016/j.compstruct.2016.01.030.
- [12] Ettbeb A. E., Rahman Z. A., Razi Idris W. M., Adam J., Rahim S. A., Ahmad Tarmidzi S. N., and Lihan T., Root tensile resistance of selected pennisetum species and shear strength of root-permeated soil. *Applied and Environmental Soil Science*, Vol. 2020, Mar. 2020, pp. 1–9, doi: 10.1155/2020/3484718.
- [13] Usifo P., and Li-Quan W., Evaluation of the biomechanical potential of pennisetum purpureum and mangifera indica plant roots for sustainable slope stabilization. *International Journal for Research in Applied Science and Engineering Technology*, Vol. 11, No. 3, Mar. 2023, pp. 604–613, doi: 10.22214/ijraset.2023.49065.
- [14] Kokutse N. K., Temgoua A. G. T., and Kavazović Z., Slope stability and vegetation: conceptual and numerical investigation of mechanical effects. *Ecological Engineering*, Vol. 86, 2016, pp. 146–153, doi: <https://doi.org/10.1016/j.ecoleng.2015.11.005>.
- [15] Mickovski S. B., and van Beek L. P. H., Root morphology and effects on soil reinforcement and slope stability of young vetiver (vetiveria zizanioides) plants grown in semi-arid climate. *Plant and Soil*, Vol. 324, No. 1, 2009, pp. 43–56, doi: 10.1007/s11104-009-0130-y.
- [16] Kusminingrum N., Peranan rumput vetiver dan bahia dalam meminimasi terjadinya erosi lereng (the role of vetiver and bahia grass in minimizing slope erosion). *Pusat Litbang Jalan dan Jembatan*, Vol. 1, No. September, 2011, pp. 1–12.
- [17] Hamdhan I. N., Anugrah R. F. V., Hulwun S., and Awalia A., Bio-engineering soil reinforcement with 3d model. *International Journal of GEOMATE*, Vol. 25, No. 110, 2023, pp. 235–242, doi: <https://doi.org/10.21660/2023.110.3906>.
- [18] Badhon F. F., Islam M. S., Islam M. A., and Arif M. Z. U., A simple approach for estimating contribution of vetiver roots in shear strength of a soil–root system. *Innovative Infrastructure Solutions*, Vol. 6, No. 2, 2021, pp. 1–13, doi: 10.1007/s41062-021-00469-1.
- [19] Shafee A., and Khoshghalb A., Particle node-based smoothed point interpolation method with stress regularisation for large deformation problems in geomechanics. *Computers and Geotechnics*, Vol. 141, Jan. 2022, p. 104494, doi: 10.1016/j.compgeo.2021.104494.
- [20] Feng K., Wang G., Huang D., and Jin F., Material point method for large-deformation modeling of coseismic landslide and liquefaction-induced dam failure. *Soil*

- Dynamics and Earthquake Engineering, Vol. 150, Nov. 2021, p. 106907, doi: 10.1016/j.soildyn.2021.106907.
- [21] Shafee A., and Khoshghalb A., An improved node-based smoothed point interpolation method for coupled hydro-mechanical problems in geomechanics. *Computers and Geotechnics*, Vol. 139, Nov. 2021, p. 104415, doi: 10.1016/j.compgeo.2021.104415.
- [22] Booth D. J., and Adinata N. A., Vetiver grass: a key to sustainable development on Bali. in *7th International Conference on Vetiver (ICV)*, Chiang Mai, Thailand, 2019.
- [23] Pusdalop BPBD Provinsi Bali, Laporan kejadian bencana Provinsi Bali 2010-2019, Denpasar.
- [24] Rusdiansyah, Adriani, Innocentia E., and Apriani R., Selection of wild plant species as soil bioengineering for soil slope stability in south kalimantan Indonesia to overcome shallow landslides. *Revista Ciencia y Construcción*, Vol. 3, No. 4, 2022, pp. 31–42.
- [25] Rahmawati N., and Lubczynski M. W., Validation of satellite daily rainfall estimates in the complex terrain of Bali island, Indonesia. *Theoretical and Applied Climatology*, Vol. 134, No. 1–2, 2018, pp. 513–532, doi: 10.1007/s00704-017-2290-7.
- [26] Rahmawati N., Space-time variogram for daily rainfall estimates using rain gauges and satellite data in mountainous tropical island of bali , indonesia (preliminary study). *Journal of Hydrology*, Vol. 590, No. February 2018, 2021, p. 125177, doi: 10.1016/j.jhydrol.2020.125177.
- [27] Mhaske S. N., Pathak K., and Basak A., A comprehensive design of rainfall simulator for the assessment of soil erosion in the laboratory. *Catena*, Vol. 172, No. September 2017, 2019, pp. 408–420, doi: 10.1016/j.catena.2018.08.039.
- [28] Carrillo N., Simple two and three dimensional case in the theory of consolidation of soils. *Journal of Mathematics and Physics*, Vol. 21, No. 1–4, 1942, pp. 1–5, doi: 10.1002/sapm19422111.
- [29] Atkinson M. S., and Eldred P. J. L., Consolidation of soil using vertical drains. *Geotechnique*, Vol. 31, No. 1, 1981, pp. 33–43, doi: 10.1680/geot.1981.31.1.33.
- [30] Abuel-Naga H., and Bouazza A., Equivalent diameter of a prefabricated vertical drain. *Geotextiles and Geomembranes*, Vol. 27, No. 3, 2009, pp. 227–231, doi: 10.1016/j.geotexmem.2008.11.006.

Copyright © Int. J. of GEOMATE All rights reserved, including making copies, unless permission is obtained from the copyright proprietors.
